SEGMENTATION OF LUNGS IN HRCT SCAN IMAGES USING PARTICLE SWARM OPTIMIZATION

Qaisar Abbas[1,2], M. Tahir Abbas Khan[3], Amjad Farooq[1,2]
and M. Emre Celebi[4]

[1]Department of Computer Science
COMSATS Institute of Information Technology
[2]Centre for Imaging and Computational Intelligence, CIIT Sahiwal
Sahiwal, Pakistan
drqaisar@ciitsahiwal.edu.pk; amjadfarooq@uet.edu.pk

[3]Ritsumeikan Asia Pacific University
1-1 Jumonjibaru, Beppu-shi, Oita 874-8577, Japan
tahir_abbas@hotmail.com

[4]Department of Computer Science
Louisiana State University
Shreveport, LA, USA
ecelebi@lsus.edu

Abstract. *A novel segmentation algorithm for lungs based on high-resolution computed tomography (HRCT) scan images is developed. This segmentation method is mainly derived from particle swam optimization (PSO) technique to select an appropriate threshold level for pixels-probability density function (P-PDF) that integrates morphological edge-detection technique to refine segmentation. A multi-level thresholding technique was proposed for CT slice segmentation by developing new control fitness function. After that morphological functions are utilized to get enhanced delineation of lungs from HRCT scan images. For computer-aided diagnostics (CADe) of lungs, this algorithm can be used as an initial step to improve the diagnostic performance of radiologists with an increase in sensitivity and decrease in false-positive (FP) rate. The system was tested on 120 HRCT scan images. This automatic thresholding method was compared with the other state-of-the-art techniques based on ground truth obtained from an expert radiologist. The experimental results indicate that the proposed method provides an effective segmentation solution with small errors, independent of CT scanners and independent from patient's low or high dose.*
Keywords: Computed tomography (CT), Lung thresholding and segmentation, Probability density function, Mixture of model, Particle swam optimization

1. **Introduction.** Lung cancer is the most common form of cancer in the United States [1], causing an estimated 222,520 new cases and 157,300 deaths in 2010. The 5-year-survival cure rate for lung cancer is about 14%, and early detection is vital to increase this rate up to 49% at stage 1, where there is a solitary, circumscribed lung nodule [2]. For early detection and diagnosis, high-resolution 3D computed tomography (HRCT) [3] is considered to be the more cost-effective and accurate imaging modality among alternatives such as chest X-ray, which is used by many radiologists. It allows detecting pathological deposits as small as 1mm in diameter that are called lung nodules. However, the detection and interpretation of lung nodules for the radiologists using HRCT scan is a tedious and difficult task, leading to a high false-negative rate and low sensitivity [4]. Therefore, Computer-aided diagnostics (CADe) [6-8] tools are developed for providing

'second opinion' to detect and classify lung tissue that may improve the radiologists' ability. Furthermore, a comparative study of CADe suggested [17] that the classification of lung tissues is still a challenging task.

The CADe of lung HRCT image consists of major three steps: (1) lung segmentation, (2) detection of candidate nodules from segmented lungs, and (3) classification of lung tissues into normal and pathological or abnormal. The effective and automatic segmentation of lungs is a vital step [18] to develop an accurate detection and classification of lung abnormalities for CADe systems. In fact, to determine an appropriate and automatic threshold value for segmentation is a critical task. Accordingly, the automatic decision of lung segmentation remains a challenging task for developing lung CADe system.

2. **Related Work and Approach.** Image processing algorithms that can be used for lung segmentation in HRCT images include fuzzy c-means clustering (FCM) and mathematical morphology [18], thresholding [19,20]. The literature review suggested that these types of segmentation algorithms provide reasonably delineated objects. However, the extraction of region-of-interest (ROI) from the segmented areas is a difficult task. As a result, other researchers have combined segmentation techniques with morphological edge-detection methods [18] to get accurate lung regions. Since, in case of medical imaging, the size of digital image is often very large, using FCM or LS techniques is very time consuming. Accordingly, an optimized thresholded technique is always required. The lung segmentation is also complicated due to the following factors: diversity of tissue volume or air volume, image acquisition protocol, physical material properties of the lung parenchyma, and transpulmonary pressure.

A novel optimal thresholding algorithm is presented based on probability density function (PDF) for lung image segmentation, and morphological functions to delineate effective lung regions from the HRCT slice. The proposed algorithm presents a multi-level thresholding technique that used particle swam optimization (PSO) technique to optimize its parameters. Furthermore, the new control fitness function is developed for PSO technique. The PDF-based [21] thresholding technique is more effective as compared to fuzzy entropy because it assigns a weighted probability to each pixel according to its corresponding class. For convenient purpose, the PDF technique is known as pixels based PDF (P-PDF) function. For thresholding, the P-PDF technique is fast due to use of PSO method and maximum likelihood criteria. The objectives of this study are to obtain more relevant, dynamic and optimal threshold value for CT image with different region segmentation. The PSO optimization technique is widely used in many application domains such as parameter tuning, 2D/3D face recognition, and image segmentation [22].

In this paper, the particle swarm global optimization is integrated into PDF-based segmentation to select the optimal parameters for thresholding, and because of its excellent performance for lung segmentation. To test the proposed algorithm, the HRCT scans images are obtained from online source [23], and other distinct sources of different patients in the form of DICOM images. In total, 120 HRCT scans images are used. The developed algorithm is compared with state-of-the-art segmentation methods: one is based on fuzzy entropy + morphology (Jaffar_fuzzy) [18] and second is based on Fuzzy entropy + Genetic (Jaffar_GeneticFuzzy) techniques with the ground truth obtained from an expert.

3. **Research Methodology.** The flow diagram of the proposed lung segmented algorithm is shown in Figure 1. The dataset acquisition is briefly described in Subsection 3.1. In Subsection 3.2, the CT scans slice is preprocessed using adaptive histogram equalization and gamma correction to enhance the contrast. The Subsections 3.3 and 3.4 represent the
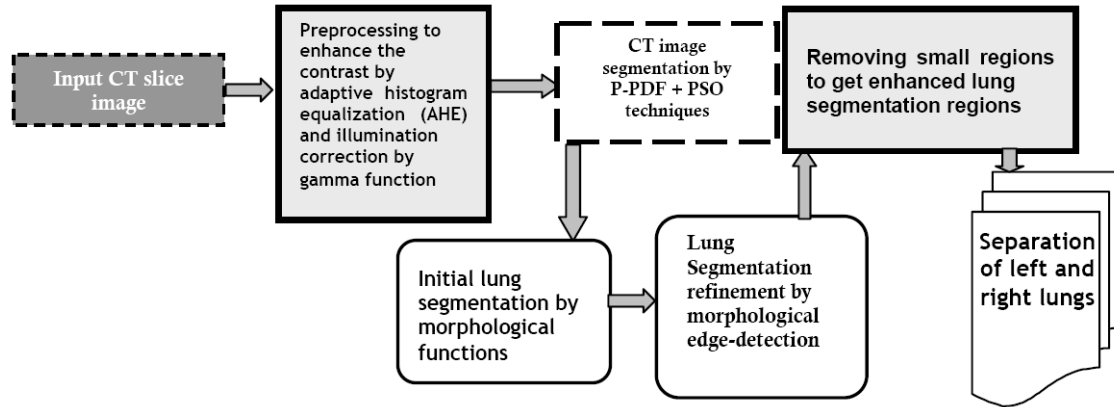
FIGURE 1. The systematic flow diagram of proposed lung HRCT scan slices segmentation algorithm

proposed method of CT image segmentation using P-PDF and PSO techniques, respectively. From this segmentation, the initial lung regions are extracted using morphological edge a detection operation, which is discussed in Subsection 3.5. In Subsection 3.6, the lung segmentation regions are refined and smoothed using image processing and morphological functions. Section 4 describes the experimental results and comparisons. The discussions of the results are in Section 5, and the paper concludes in Section 6.

3.1. **Dataset acquisition.** To test the lung segmentation algorithm, a dataset of HRCT scans were acquired from different online sources, but mostly the images came from the Lung Imaging Database Consortium (LIDC) [23]. 48 scans of different subjects are included in this dataset. Each of these scans contained a number of image slices. In total, 80 slices have selected from the 48 scans that also contained nodule pattern information. The images in this dataset were of size 512×512 stored in the DICOM format. The size of pixel ranged from 0.488mm to 0.762mm, and also the thickness of a slice varied from 2.0mm to 3.0mm. In this dataset, the 80 images are extracted from each patient with low-dose. Moreover, the 40 remaining images are obtained with high-dose and different scanners. As a result, the total 120 images are used in order to evaluate the segmentation results. To measure the performance, the boundaries of both lungs of 120 scans are manually marked by an expert radiologist, which serves as a gold standard.

3.2. **Preprocessing.** To improve the visual quality of HRCT scan images, the preprocessing step is performed by using adaptive histogram equalization (AHE) [24], gamma correction [25] techniques. Due to acquisition devices used in HRCT scanning, the brightness is not sufficient and noise is also presented in the images that may adversely affect the segmentation process. To enhance the image quality, the AHE technique is applied. In AHE method, the image is divided into 16×16 sub-regions, and histogram equalization is applied to each one of them. In practice, it modifies the intensity values using a nonlinear methodology for maximizing the contrast for all regions of the image. As a result, inconspicuous features become more visible. However, it may modify the brightness of the image. Once AHE was applied, gamma correction procedure is applied sequentially to improve the brightness of the overall image. Next, the CT scans is segmented and lung regions are extracted.

3.3. **CT image segmentation.** After preprocessing the CT slice image, the segmentation is performed to convert it into a binary image by using pixels-probability density function (P-PDF), and its parameters are optimized by particle swarm optimization (PSO).

The goal of this step is to separate body regions from the background into mainly three parts: fat, other tissues (including bone, organ, vessels, and so on) and air-filled regions. A multi-level grayscale thresholding method is used to identify the regions based on their respective density distributions. Instead of using fixed threshold values to segment target regions, our technique uses a histogram analysis method that determine the optimal and dynamic threshold value for the CT slice automatically.

The determination of optimal threshold value for segmenting chest body regions from the background that is almost filled by air is a difficult task. The three parts of a CT image consist of regions with different intensity distributions. Mixture model or class based segmentation [21] approach is widely used in many applications in practice that try to identify the probabilities of pixels, which can be modeled to find the probability of any pixel value belonging to distinct classes or regions. It is basically derived from PDF based estimation that takes into account histogram of an image to perform segmentation step. Usually, the histogram of an image provides a scheme about the PDF of pixel values. For instance, a grayscale CT image consists of 256 intensity values, and it is apparent that the histogram bin centers at $0, 1, \ldots, Lv = 255$ should be defined. An overall mixture of the model for the PDF of pixels values could be derived from this histogram to model the segmentation of CT slice.

Let x be the pixel value of the corresponding histogram and $f(x)$ be probability for that pixel. Then, $f(x)$ can be defined as in terms of conditional probability.

$$P_{prob}(x|\text{Cl}_i) = P_{prob}(\text{Cl}_i) f_i(x|\text{Cl}_i) \tag{1}$$

where P_{prob} represents probability, $P_{prob}(\text{Cl}_i)$, $i = 1, 2, \ldots, k$ being class prior probabilities and $f_i(x|\text{Cl}_i)$ represent the class conditional PDF of x. Then, $f(x)$ becomes

$$f(x) = P_{prob}(\text{Cl}_1) f_1(x|\text{Cl}_1) + \ldots + P_{prob}(\text{Cl}_k) f_k(x|\text{Cl}_k) \tag{2}$$

It should be noticed from Equation (2) that the PDF, i.e., $f(x)$ can be represented as a weighted sum of k class conditional PDFs and weights (w_i) are being the class prior probabilities $P_{prob}(\text{Cl}_i)$. Thus, Equation (2) can be simply rewritten as:

$$f(x) = \sum_{i=1}^{k} w_i f_i(x|\theta_i) \tag{3}$$

Here, $f_i(x|\text{Cl}_i)$ is replaced by $f_i(x|\theta_i)$, for the reason that each class conditional PDF is known with θ_i parameters. In this segmentation technique, normal mixture components are utilized, and then $f_i(x|\theta_i)$ can be written as:

$$f_i(x|\theta_i) = N(x|\boldsymbol{\mu_i}, \sigma_i) = (2\pi)^{-d/2} |\sigma_i|^{-1/2} \exp\left\{-(x - \boldsymbol{\mu_i})^T \sigma_i^{-1} (x - \boldsymbol{\mu_i})/2\right\} \tag{4}$$

where $f_i(x|\theta_i)$ is component of ith model, θ_i is the vector of all unknown parameter, μ_i is the mean and σ_i is the covariance matrix. In order to validate a $f(\mathbf{x})$ of PDF, $\sum_{i=1}^{k} w_i = 1$ must be fulfilled, where k indicates components of densities. As a result, Equation (4) is used to determine the probabilities of each class the pixels belong to. If we assume that this observation in the data set is independent, the maximum likelihood function $l(\boldsymbol{\theta})$ can be derived from this assumption to show the joint probability. The joint probability of having a particular set of observations is written as:

$$l(\boldsymbol{\theta}) = l(\mathbf{x}_1, \mathbf{x}_2, \ldots, \mathbf{x}_n|\theta) = P_{prob}[\cap_{j=1}^{n} \mathbf{x}_j | \boldsymbol{\theta}] = \prod_{j=1}^{n} f(\mathbf{x}_j|\boldsymbol{\theta}) \tag{5}$$

where $f(\mathbf{x}_j|\boldsymbol{\theta}) = \sum_{i=1}^{k} w_i f_i(\mathbf{x}_j|\boldsymbol{\theta}_i)$. In the PDF mixture of models, there are many ways to determine unknown parameters, but the easiest way is to select $\boldsymbol{\theta}$ in such a way that

it maximizes the likelihood function $l(\boldsymbol{\theta})$. The maximum likelihood (ML) estimate of $\boldsymbol{\theta}$ can be written as:

$$\boldsymbol{\theta}_{ML} = \arg_{\boldsymbol{\theta}} \max l(\boldsymbol{\theta}) \tag{6}$$

To determine $\boldsymbol{\theta}$ in the sense of ML estimation, the set of $\mu_{\mathbf{i}}$, $\sigma_{\mathbf{i}}$ and $w_{\mathbf{i}}$ must be optimized. Therefore, the vector of all unknown parameters can be combined represent by the Equation (7) as:

$$\alpha = (w_M \boldsymbol{\theta})^T \text{ or } \alpha = (w_1 \mu_1 \sigma_1, w_2 \mu_2 \sigma_2, \ldots, w_M \mu_M \sigma_M)^T \tag{7}$$

The limit for determining the unknown parameters are defined by $3M - 1$ that used ML estimator to a threshold the lung CT image. In order to segment the CT image, the two-level threshold value is considered overall lung region segmentation. Learning the mixture, namely, estimating the weights w_i and the parameters θ_i of each component is often carried out using expectation maximization (EM) algorithm. However, there are some limitations of EM algorithm: it considers that the mixing components are known, there is no commonly accepted superior method for parameter's initialization, and the method is of local nature and consequently, can get in local maxima of the likelihood function. Accordingly, it is difficult to determine and optimize unknown parameters by EM algorithm. Therefore, the PSO technique is utilized that integrates a new fitness function using the Jensen-Shannon divergence measures. For optimization of parameters, GA is widely used. Even so, as compared to GA, PSO does not employ filtering; specifically, all members in the population survive during the entire search process.

3.4. **Optimization.** The PSO-based optimization technique is based on each individual particle in the swarm is composed of three dimensional vectors in the search space. In the three dimensional vectors, the current position is denoted by a vector s_i, the previous best position is p_i, and the velocity is v_i. The first vector s_i is considered as a set of coordinates represents a point in search domain. During iteration of PSO algorithm, the recent position is evaluated as a problem solution. If that position is better than other, then the coordinates are stored in the vector p_i. The function result is provided the best value is stored in $pbest_i$ for previous best and for later on iterations comparisons. Generally, the main reason is to keep searching the better positions and changing p_i and $pbest_i$ vectors. After that new points are selected by inserting v_i coordinates to s_i and the technique is operated by adjusting v_i, which was seen as a step size. If the search space is D-dimensional vector, the ith particle of the population or swarm can be denoted by the vector $S_i = (s_{i1}, s_{i2}, \ldots, s_{iD})^T$, the velocity of the particle can be represented as $V_i = (v_{i1}, v_{i2}, \ldots, v_{iD})^T$ and the best possible visited position is $P_i = (p_{i1}, p_{i2}, \ldots, p_{iD})^T$. Then the swarm is updated according to:

$$v_{id}^{n+1} = \omega[\beta\, v_{id}^n + c_1 r_1^n (p_{id}^n - s_{id}^n)/\Delta t + c_2 r_2^n (p_{gd}^n - s_{id}^n)] \tag{8}$$

and

$$s_{id}^{n+1} = s_{id}^n + \Delta t\, v_{id}^{n+1} \tag{9}$$

where g is defined as the index of the large-scale lead of the particle in the swarm, and $d = (1, 2, \ldots, D)$ is represented the iterations, N is the size of population; ω is a constriction factor which controls and constricts the velocity's magnitude; β is the inertial weight. This weight is repeatedly used to manage the investigation and operation in the search space. The parameters c_1 and c_2 are positive constants called acceleration coefficients; r_1 and r_2 are random numbers, uniformly distributed in $[0, 1]$; Δt is the iteration number. The steps for implementing PSO algorithm are summarized below:

(1) Initialize particle s_i with random positions and velocities v_i on D-dimensions.

(2) For every particle, evaluate the following proposed effective fitness function in D variables.

To find best fitness function for PSO, the average histogram of pixels distribution is used, which is also defined by P-PDF technique, which is calculated by Equation (10) as:

$$P_{pixels}(i) = \frac{1}{N} \sum_{i=1}^{Lv} H(i) \tag{10}$$

To measure the strength of pixels on each grayscale level (Lv), The JSD (Jensen-Shannon divergence) statistical measure was integrated to the fitness function that indicated the degree of apart from the pixels histogram to the corresponding weighted probability, which was calculated by $f_i(s|\theta_i)$. The JSD is given as follows:

$$D_{JSD}\left(f(s|\theta), P'_{pixel}\right) = \sum_{i=1}^{Lv} f_i(s|\theta_i) \log \frac{2f_i(s|\theta_i)}{f_i(s|\theta_i) + P'_{pixel}} + P'_{pixel} \log \frac{2P'_{pixel}}{P'_{pixel} + f_i(s|\theta_i)} \tag{11}$$

Then calculate the weighted probability of each pixel through the P-PDF and velocities as:

$$\eta(s_i\,|\alpha) = \sum_{i=1}^{k} P_{pixels}(i) \times \sum_{i=1}^{k} w_i f(s_j|v_i) \tag{12}$$

And finally, the objective fitness function is derived as:

$$obj(i) = 1 - \left((D_{JSD}(f(s|\theta), P'_{pixel} - \eta(s_i\,|\alpha)) + \mu_i\right)/\sigma_i \tag{13}$$

(3) Compare this fitness evaluation function with its $pbest_i$. This comparison is based on the condition that if recent value is superior than $pbest_i$, then $pbest_i$ is equal to this value and p_i equal to the current location s_i.

(4) Recognize the swarm particles in the neighborhood so far with the good success, and allocate its index to g.

(5) Update the set of velocities and the positions of the swarm particle by following the Equation (14).

$$\left\{ \begin{array}{l} \vec{v}_i \leftarrow \vec{v}_i + \vec{U}(0, \phi_1) \otimes (\vec{p}_i - \vec{s}_i) + \vec{U}(0, \phi_2) \otimes (\vec{p}_g - \vec{s}_i), \\ \vec{s}_i \leftarrow \vec{s}_i + \vec{v}_i \end{array} \right\} \tag{14}$$

where $\vec{U}(0, \phi_1)$ represents the random numbers created at each iteration step and for every particle and $\otimes$ is component-wise multiplication operator.

(6) If the good fitness function or iterations criterion is met then, return function.

(7) If it is not then again goto step **(2)**.

Once the unknown parameters are determined and optimized by PSO, then an assignment of each pixel to different classes can be estimated by using maximum likelihood criterion. The above steps of PSO algorithm are iterated (i.e., repeat the expectation and maximization steps) until the changes in the mixture parameter are smaller than a tolerance level or maximum number of iterations is reached. In our application, the tolerance parameter and the maximum iteration are set as 0.00001 and 230, respectively. This is the final thresholding step to partition CT slice into different regions (chest body air surrounding, the lungs, and other low-density regions). However, to retain just chest CT scan area, unwanted objects are filtered out. For this purpose, connected components (CC)-labeling algorithm is utilized to recognize the lung voxels. To remove background air, those pixels are deleted that are connected to the border of the image. Small, disconnected areas are erased if the region area is too small, or it has been low-density that are presented outside the lung regions.

3.5. **Initial lung segmentation.** After applying the optimal and dynamic threshold value with CC-labeling algorithm, the CT slice image is segmented into different parts such as lungs and chest regions. However, we are interested to obtain accurate lung regions that will be further utilized for identification of lung disease patterns. To segment lung regions, first a chest regional mask was obtained using morphological image filling function that also eliminates the interior cavities. However, this image is also contained other regions that must be removed as indicated by red lines. Therefore, to select a chest regional mask than other objects, a binary image selection function is performed to get a binary image containing the objects that overlap the pixel from the center point with 8-connected pixels value. Next, a simple bitwise AND ($\&$) operation is performed to obtain initial lung area segmentation between segmented CT slice image (St), and inverse of obtained chest regional mask that is given by:

$$Lung\_regions = region\_mask \,\&\, (\sim St) \qquad (15)$$

From this operation, the chest region is divided into the left and right lungs but may be due to weak anterior and posterior junction points or diffuse muscle areas so it is very difficult to separate two lungs. The objective of the lung separation step is to find these junctions lines and entirely split the right and left lungs. For this purpose, the center point is used and scans the lung regions. From the maximum points in the y-direction, the lungs are divided into two parts if the lung region has only one region. After that morphological area filling operation is performed again to fill the lung regions. The roughness of the segmented region may be occurred due to bronchial airways tree or tissue patterns inside the lung regions. Accordingly, a refinement of lung segmentation results is necessary.

3.6. **Lung segmentation refinement.** This refinement step uses functions from mathematical morphology to address three shape-related problems: boundary indentations caused by the large pulmonary vessels; large boundary bulges caused by the left and right main-stem bronchi merging into the lungs; and small boundary bulges caused by small airways near the lung borders. In this step, left and right contour of lungs are used. First, initialize the structure element (SE) = 10 and disk = SE/6 parameters for this operation. By using morphological area opening function and CC_Labeling algorithm, the objects having the area of 100 pixels are separated from the lung mask. Afterwards, the whole connected objects are scanned in both images to find the areas of each object. Next, determine the first and second largest connected object areas and positions to get left and right lungs. This process is generated left and right lung masks. At last, smooth left and right lungs are obtained by applying morphological opening, filling and erode functions. This was the step in HRCT lung image segmentation that can be used to improve the performance level of CADe systems.

4. **Results.** The proposed segmentation algorithm was evaluated using 120 HRCT images of size 512×512 pixels stored in the DICOM format. For performance comparisons, all images are first preprocessed to enhance the HRCT images and then statistical metric were used to quantify the effectiveness of segmentation. To assess the segmentation accuracy, the automatic computer-based algorithm was compared with the results obtained by manual ground truth obtained from an expert radiologist (over 12 years of experience). Each scan HRCT image slice, the radiologist manually determined the outlines of each left and right lung borders on this dataset. Overall in this dataset, 240 border images are obtained from the left and right lung borders on 120 slices. The comparisons between automatic segmentation and manual tracing are performed using the Hammoude distance (HD). The HD statistical metric makes a pixel by pixel comparison in such a way that each pixel classified as lung boundary by the radiologist that were not classified as such by

the computer-based automatic segmentation and pixels classified as lung boundary by the automatic segmentation. It means the greater the HD value of automatic segmentation (A) than manually tracing (B), the lower the segmentation accuracy. The HD metric is defined as:

$$HD = (\#(A \cup B) - \#(A \cap B)/\#(A \cup B)) \qquad (16)$$

where $\#$ denotes the number of pixels. The mean, average, minimum, maximum and standard deviation statistics are derived from this HD metric on 120 HRCT slices (total 240 lung images).

The comparison result on this dataset between automatic and manual segmentation is represented in Table 1. On median and average segmentation errors are obtained on both lungs (LL: 9.17, LL: 8.30) and (RL: 11.13, RL: 9.47), respectively. The lung border segmentation error of right lung-region is high in every case. This is due to reason that it is very difficult to segment RR region because of diffuse tissue patterns or bronchi tree in the right lung areas when observed in this dataset. However, the mean and standard deviation for both LL and RL border errors were obtained, i.e., 8.10 $\pm$ 4.27 and 9.12 $\pm$ 5.14, respectively.

In order to test generality of the automatic segmentation algorithm for HRCT slices, experiments on different type of image have performed that are captured from different scanners. Figure 2 shows a comparison between the manually identified lung regions and the computer-based detected borders. This figure represents the actual difference between the observer and the computer. From Figures 2(a), 2(b) and 2(c), it can be noticed that the automatic segmentation can effectively segment lung regions. The detected regions are indicated by red contours.

TABLE 1. Comparison results of computer-based and manual segmentation using HD metric

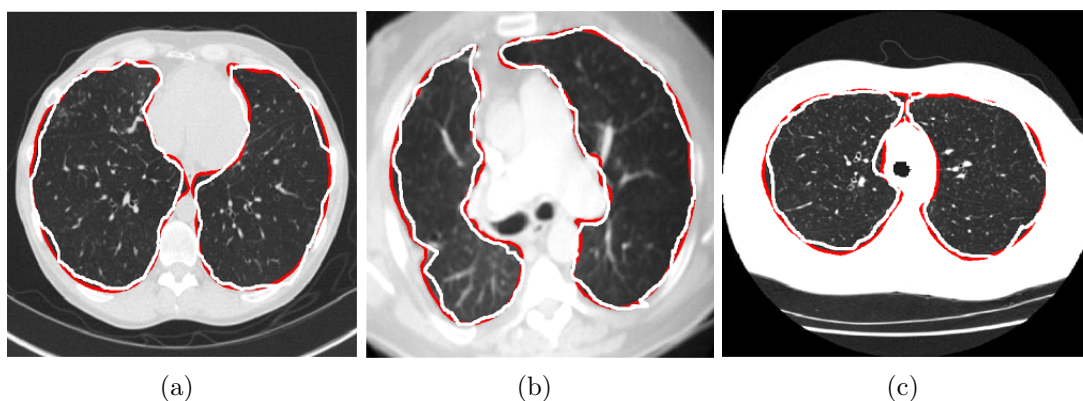| Method	Median	average	Mean $\pm$ Standard deviation	Minimum	Maximum
Left Lung (LL) segmentation	9.17	8.30	8.10 $\pm$ 4.27	0.24	11.65
Right lung (RL) segmentation	11.13	9.47	9.12 $\pm$ 5.14	1.58	15.20

(a)　　　　　　　　(b)　　　　　　　　(c)

FIGURE 2. An example of comparison between automatic and manual lung segmentation algorithm, where red outlines indicate compare-based segmentation, and white contour indicate manual border drawn by an expert radiologist

To perform a comparative study with the state-of-the-art lung segmentation techniques, the Jaffar_fuzzy [18] and Jaffar_Geneticfuzzy algorithms are implemented and tested on this dataset using HD metric. The comparisons results of the proposed method and two other are represented in Table 2. From Table 2, the proposed system is achieved lowest segmentation errors as compared to Jaffar_fuzzy and Jaffer_Geneticfuzzy methods. This shows that the significant segmentation results are obtained through a propose system.

TABLE 2. Comparisons with the state-of-the-art lung segmentation techniques with the proposed method using HD metric

Method	Mean ± Standard deviation (LL)[1]	Mean ± Standard deviation (RL)[2]
Jaffar_fuzzy [18]	21.35 ± 10.90	24.13 ± 13.11
Jaffar_Geneticfuzzy	17.14 ± 9.20	20.47 ± 10.55
Proposed (P-PDF+PSO + morphology)	8.10 ± 4.27	9.12 ± 5.14

[1]Left Lung = LL, [2]Right Lung = RL

5. **Discussion.** Accurate lung segmentation in HRCT scan images is essential to detect and classify disease tissue patterns. The segmentation step of HRCT scan images is difficult due to diversity of tissue volume or air volume, image acquisition protocol, physical material properties of the lung parenchyma, and transpulmonary pressure. If the state-of-the-art segmentation algorithms such as thresholding, edge detection and level set based are applied to delineate the lung regions for HRCT scan images, then these factors often influence the results. Due to different factors present in HRCT scan images, it is required to set up different threshold values or parameters.

An optimal and dynamic threshold value for all HRCT scan images is difficult to find out. Therefore, this paper makes use of pixels based probability density functions (P-PDF) to determine the class each pixel belongs to. The parameters of P-PDF are optimized by particle swarm optimization (PSO) algorithm. In this PSO algorithm, the effective fitness function is developed to control the convergence of the model. This threshold (P-PDF + PSO) technique provides an optimal and dynamic threshold value based on pixels probability weight. In addition, morphological operations are performed to effectively segment the lung regions. Prior to segmentation, the image is enhanced using AHE and gamma correction techniques.

The comparison between computer-based automatic segmentation is performed with manual border traced by an expert radiologist. Figure 2 displays the overall computer-based and manual tracing lung segmentation results. In order to do performance analysis, the Hammoude distance (HD) metric is computed with statistical median; average; mean; standard deviation; minimum and maximum characteristics. The results were tested on 120 HRCT scan slices captured from different scanners. The minimum segmentation errors are 0.24 and 1.58 for left and right lungs, respectively. To evaluate the performance of the proposed system, the comparisons with Jaffar_fuzzy [18] and Jaffar_Geneticfuzzy algorithms are also performed. In order to use Entropy [18] or Fuzzy entropy with Genetic algorithm, a threshold value is obtained, which is not suitable for determining the accurate regions of both left and right lungs in HRCT scans images. Compared with other optimization techniques such as GA, the PSO algorithms are provided less search time in the segmentation, and also have good search stability in the repeated experiments. As mentioned before, PSO does not employ filtering; specifically, all members in the population survive during the entire search process as compared to GA. An integration of PSO and obtained segmentation result indicates that this method is highly accurate and it can

potentially be used to classify normal and abnormal lung disease patterns as compared to state-of-the-art techniques.

6. **Conclusion.** This paper presents a novel segmentation algorithm for lungs based on high-resolution computed tomography (HRCT) scan images. This algorithm contained two major parts: (1) preprocessing to enhance the HRCT scan images, and (2) lung region segmentation. To preprocess the HRCT scan slice, the HE and gamma correction techniques are utilized. In order to achieve effective lung segmentation after preprocessing, the pixels-probability density function (P-PDF) is calculated, and its parameter are optimized by a particle swam optimization (PSO) technique. In the PSO process, a new control fitness function is also integrated based on divergence measure. This technique is used to segment the whole CT slice into different regions. However, to select left and right lung regions, morphological operations are used. The advantage of using proposed segmentation algorithm is that the lung region detection results are not affected by diversity of tissue volume or air volume, image acquisition protocol, physical material properties of the lung parenchyma, and transpulmonary pressure. Regardless of the type of scanner, it can effectively segment both lung regions with low errors. In contrast to the state-of-the-art segmentation techniques, it is not based on a single threshold value for all type of images. This segmentation algorithm is based on a dynamic and optimal thresholding technique.

This segmentation algorithm could be used as an initial step to improve the diagnostic performance of radiologists with a high sensitivity and a low false-positive (FP) rate for developing computer-aided diagnostics (CADe) of lungs. This algorithm was tested on 120 HRCT scan images obtained from diverse sources, and ground truth obtained from an expert radiologist. The comparisons results with the ground truth data and state-of-the-art techniques show that this method provides an effective segmentation solution.

Although, the conducted experiments suggest that this algorithm provides effective lung segmentation results in CT scan images. It may provide erroneous segmentation results if a large portion of patient's lung was filled with large opacities in a way that the opacity connects cross borders of lung together. As future work, we will extend our algorithm to use lung or anatomical knowledge to overcome this drawback. We also plan to detect and classify normal and abnormal lung tissues.

REFERENCES

[1] A. Jemal, R. Siegel, J. Xu and E. Ward, Cancer statistics, *CA Cancer J. Clin.*, vol.60, no.5, pp.277-300, 2010.

[2] J. V. Forrest and P. J. Friedman, Radiologic errors in patients with lung cancer, *Western J. Med.*, vol.134, no.6, pp.485-490, 1981.

[3] C. I. Henschke et al., Early lung cancer action project: Overall design and findings from baseline screening, *Lancet*, vol.354, no.9173, pp.99-105, 1999.

[4] H. MacMahon, J. H. M. Austin, G. Gamsu, C. J. Herold, J. R. Jett, D. P. Naidich et al., Guidelines for management of small pulmonary nodules detected on CT scans: A statement from the Fleischner society, *Radiology*, vol.237, no.2, pp.395-400, 2005.

[5] S. J. Swensen, J. R. Jett, T. E. Hartman, D. E. Midthun, J. A. Sloan et al., Lung cancer screening with CT: Mayo clinic experience, *Radiology*, vol.226, pp.756-761, 2003.

[6] I. C. Sluimer, A. M. R. Schilham, M. Prokop et al., Computer analysis of computed tomography scans of the lung: A survey, *IEEE Trans. on Medical Imaging*, vol.25, no.4, pp.385-405, 2006.

[7] T. W. Way, B. Sahiner, H. P. Chan, L. Hadjiiski et al., Computer-aided diagnosis of pulmonary nodules on CT scans: Improvement of classification performance with nodule surface features, *Med. Phys.*, vol.36, no.7, pp.3086-3098, 2009.

[8] T. Messay, R. C. Hardie and S. K. Rogers, A new computationally efficient CAD system for pulmonary nodule detection in CT imagery, *Med. Image Anal.*, vol.14, no.3, pp.390-406, 2010.

[9] A. P. Reeves, A. B. Chan, D. F. Yankelevitz et al., On measuring the change in size of pulmonary nodules, *IEEE Trans. Med. Imaging*, vol.25, no.4, pp.435-450, 2006.

[10] J. W. Gurney and S. J. Swensen, Solitary pulmonary nodules: Determining the likelihood of malignancy with neural network analysis, *Radiology*, vol.196, pp.823-829, 1995.

[11] Y. Kawata, N. Niki, H. Ohmatsu, R. Kakinuma et al., Quantitative surface characterization of pulmonary nodules based on thin-section CT images, *IEEE Trans. Nucl. Sci.*, vol.45, no.4, pp.2132-2138, 1998.

[12] M. F. McNitt-Gray, E. M. Hart, N. Wyckoff, J. W. Sayre et al., A pattern classification approach to characterizing solitary pulmonary nodules imaged on high resolution CT: Preliminary results, *Med. Phys.*, vol.26, no.6, pp.880-888,1999.

[13] T. W. Way, L. M. Hadjiiski, B. Sahiner, H.-P. Chan, P. N. Cascade et al., Computer-aided diagnosis of pulmonary nodules on CT scans: Segmentation and classification using 3D active contours, *Med. Phys.*, vol.33, no.7, pp.2323-2337, 2006.

[14] K. Suzuki, S. G. Armato, F. Li, S. Sone and K. Doi, Massive training artificial neural network (MTANN) for reduction of false positives in computerized detection of lung nodules in low-dose computed tomography, *Med. Phys.*, vol.30, no.7, pp.1602-1617, 2003.

[15] Y. Uchiyama, S. Katsuragawa, H. Abe, J. Shiraishi et al., Quantitative computerized analysis of diffuse lung disease in high-resolution computed tomography, *Med. Phys.*, vol.30, no.9, pp.2440-2454, 2003.

[16] I. C. Sluimer, P. F. van Waes, M. A. Viergever et al., Computer-aided diagnosis in high resolution CT of the lungs, *Med. Phys.*, vol.30, no.12, pp.3081-3090, 2003.

[17] B. van Ginneken, S. G. Armato, B. de Hoop et al., Comparing and combining algorithms for computer-aided detection of pulmonary nodules in computed tomography scans: The ANODE09 study, *Med. Image Anal.*, vol.14, no.6, pp.707-722, 2010.

[18] M. A. Jaffar, A. Hussain and M. M. Anwar, Fuzzy entropy and morphology based fully automated segmentation of lungs from CT scan images, *International Journal of Innovative Computing Information and Control*, vol.5, no.12(B), pp.4993-5002, 2009.

[19] M.-H. Horng and T.-W. Jiang, Multilevel image thresholding selection based on the firefly algorithm, *ICIC Express Letters*, vol.5, no.2, pp.557-562, 2011.

[20] F. Nie, C. Gao, Y. Guo and M. Gan, Tsallis cross entropy based automatic threshold selection, *ICIC Express Letters*, vol.4, no.3(B), pp.993-998, 2010.

[21] C. Nikou, N. P. Galatsanos and A. C. Likas, A class-adaptive spatially variant mixture model for image segmentation, *IEEE Trans. Image Process*, vol.16, no.4, pp.1121-1130, 2007.

[22] M. Maitra and A. Chatterjee, A hybrid cooperative-comprehensive learning based PSO algorithm for image segmentation using multilevel thresholding, *Expert Systems with Applications*, vol.34, no.2, pp.1341-1350, 2008.

[23] G. A. Samuel, M. Geoffrey, F. Michael et al., Lung image database consortium: Developing a resource for the medical imaging research community, *Radiology*, vol.232, no.3, pp.739-748, 2004.

[24] J. A. Stark, Adaptive image contrast enhancement using generalizations of histogram equalization, *IEEE Trans. Image Process*, vol.9, no.5, pp.889-896, 2000.

[25] H. Farid, Blind inverse correction, *IEEE Trans. Image Process*, vol.10, pp.1428-1433, 2001.